

Journal Pre-proof

pH titration of β -lactoglobulin monitored by laser-based Mid-IR transmission spectroscopy coupled to chemometric analysis

Andreas Schwaighofer, Mirta R. Alcaraz, Laurin Lux, Bernhard Lendl



PII: S1386-1425(19)31026-1

DOI: <https://doi.org/10.1016/j.saa.2019.117636>

Reference: SAA 117636

To appear in: *Spectrochimica Acta Part A: Molecular and Biomolecular Spectroscopy*

Received Date: 10 July 2019

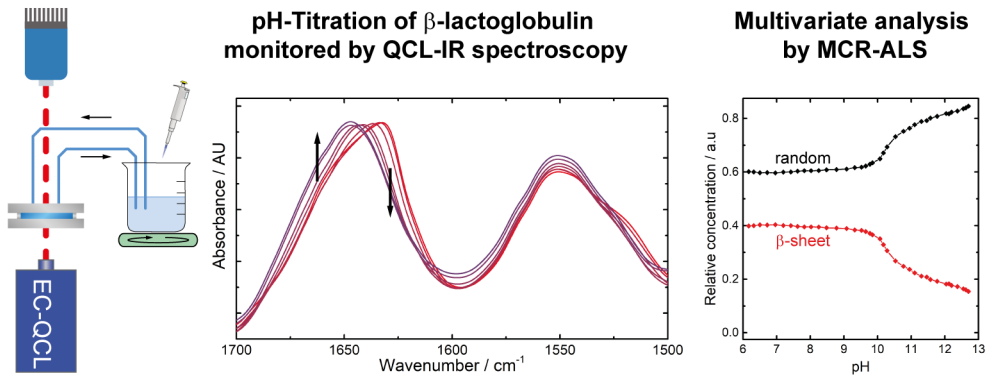
Revised Date: 27 September 2019

Accepted Date: 7 October 2019

Please cite this article as: A. Schwaighofer, M.R. Alcaraz, L. Lux, B. Lendl, pH titration of β -lactoglobulin monitored by laser-based Mid-IR transmission spectroscopy coupled to chemometric analysis, *Spectrochimica Acta Part A: Molecular and Biomolecular Spectroscopy* (2019), doi: <https://doi.org/10.1016/j.saa.2019.117636>.

This is a PDF file of an article that has undergone enhancements after acceptance, such as the addition of a cover page and metadata, and formatting for readability, but it is not yet the definitive version of record. This version will undergo additional copyediting, typesetting and review before it is published in its final form, but we are providing this version to give early visibility of the article. Please note that, during the production process, errors may be discovered which could affect the content, and all legal disclaimers that apply to the journal pertain.

© 2019 Published by Elsevier B.V.



Journal Pre-proof

1 **pH Titration of β -Lactoglobulin Monitored by Laser-based Mid-IR**
2 **Transmission Spectroscopy coupled to Chemometric Analysis**

3
4
5 Andreas Schwaighofer¹, Mirta R Alcaraz^{2,3,4}, Laurin Lux¹, Bernhard Lendl^{1,*}

6
7
8 ¹ Institute of Chemical Technologies and Analytics, Vienna University of Technology,
9 Getreidemarkt 9/164-UPA, 1060 Vienna, Austria

10
11 ² Laboratorio de Desarrollo Analítico y Quimiometría (LADAQ), Cátedra de Química Analítica
12 I, Facultad de Bioquímica y Ciencias Biológicas, Universidad Nacional del Litoral, Ciudad
13 Universitaria, Santa Fe (S3000ZAA), Argentina

14
15 ³ Departamento de Química Inorgánica, Analítica y Química Física, INQUIMAE, Facultad de
16 Ciencias Exactas y Naturales, Universidad de Buenos Aires, Intendente Güiraldes 2160, Ciudad
17 Universitaria, Pabellón 2, Buenos Aires (C1428EGA), Argentina

18
19 ⁴ Consejo Nacional de Investigaciones Científicas y Técnicas (CONICET), Godoy Cruz 2290
20 CABA (C1425FQB), Argentina.

21
22 *Corresponding author: Email: bernhard.lendl@tuwien.ac.at

24 **Abstract**

25 A novel external cavity-quantum cascade laser (EC-QCL)-based setup for mid-IR transmission
26 spectroscopy in the amide I and amide II region was employed for monitoring pH-induced
27 changes of protein secondary structure. pH titration of β -lactoglobulin revealed unfolding of
28 the native β -sheet secondary structure occurring at basic pH. Chemometric analysis of the
29 dynamic IR spectra was performed by multivariate curve resolution-alternating least squares
30 (MCR-ALS). Using this approach, spectral and abundance distribution profiles of the
31 conformational transition were obtained. A proper post-processing procedure was implemented
32 allowing to extract information about pure protein spectra and spurious signals that may
33 interfere in the interpretation of the system. This work demonstrates the potential and versatility
34 of the EC-QCL-based IR transmission setup for flow-through applications, benefitting from the
35 high available optical path length.

36
37 **Keywords:** mid-infrared, quantum cascade laser, protein structure, pH titration, β -lactoglobulin,
38 chemometrics

39

40

41 1. Introduction

42 Mid-infrared (mid-IR) spectroscopy is a powerful and well-established analytical
43 technique to study the structure of biological macromolecules, e.g., proteins [1]. Vibrations of
44 the polypeptide repeating units of proteins result in nine characteristic group frequencies in the
45 mid-IR region referred to as amide bands. For investigation of the protein secondary structure,
46 the amide I ($1700\text{-}1600\text{ cm}^{-1}$ – originating from the C=O stretching and N–H in-phase bending
47 vibration of the amide group) and the amide II bands ($1600\text{-}1500\text{ cm}^{-1}$ – arising from N–H
48 bending and C–N stretching vibrations) have been recognized to be most characteristic to
49 secondary structure [1,2]. The sensitivity to individual secondary structure elements originates in
50 differing patterns of hydrogen bonding, dipole-dipole interactions and geometric orientations in
51 the α -helices, β -sheets, turns and random coil structures that induce different frequencies of the
52 C=O vibrations [3]. Although the amide I band demonstrates to be most sensitive to
53 conformational changes, it has been shown that additional and more in-depth information about
54 protein secondary structure can be gained by collective analysis of both spectral regions,
55 particularly in combination with chemometric analysis [4-6].

56 An experimental limitation to investigations of protein secondary structure in aqueous
57 solutions with state-of-the-art Fourier transform infrared (FTIR) spectrometers is constituted by
58 the low feasible path lengths of the transmission cells. This constraint originates from the
59 combination of two factors: first, the HOH-bending band of water near 1645 cm^{-1} with a high
60 molar absorption coefficient, which overlaps with the protein amide I band; and second, the low
61 emission power provided by conventional thermal light sources (globars). As a consequence,
62 path lengths most commonly used for IR transmission measurements of proteins in aqueous
63 solutions are in the range of $8\text{ }\mu\text{m}$ to avoid total IR absorption in the region of the HOH-bending
64 band. This limitation comes along with laborious cell and sample handling as well as the need

65 for high protein concentration ($>10 \text{ mg mL}^{-1}$) [7]. The low feasible path lengths for FTIR
66 transmission measurements of proteins in aqueous solution are a considerable impairment for the
67 robustness of analysis and impede flow-through measurements and high-throughput applications.
68 This prevents semi-automated measurements in process analytical applications, but also basic
69 monitoring of titrations in transmission mode to follow conformation changes of proteins as a
70 function of external perturbation (pH, ligand concentration, denaturant concentration, etc) [8].

71 With the introduction of quantum cascade lasers (QCL) a significant step forward was
72 made towards resolving these restrictions of low power light sources in mid-IR spectroscopy [9].
73 They provide polarized and coherent light with spectral power densities several orders of
74 magnitude higher than thermal light [10]. Initially, the advantages of this new light source were
75 predominantly exploited in the gas phase and custom-built setups have gained manifold
76 implementations in process analytical applications as well as in biomedical spectroscopy [11]. In
77 the last decade, a new type of these mid-IR lasers, external cavity-QCLs (EC-QCLs), became
78 commercially available combining high emission powers with spectral tuning ranges of several
79 hundred wavenumbers. The high available emission powers enabled to increase the optical path
80 up to $38 \mu\text{m}$ for transmission measurements in the protein region [12]. EC-QCL-based IR
81 transmission measurements have been successfully accomplished for the analysis of protein
82 secondary structure [13-15]. Furthermore, the feasibility of protein discrimination and
83 quantitation in commercial bovine milk samples has been demonstrated by QCL-IR spectroscopy
84 and evaluation of the amide I band using partial least squares (PLS) modelling [16-18]. Recently,
85 an EC-QCL-based IR transmission setup was introduced for the analysis of the protein amide I
86 and II regions, which favourably competes with FTIR spectroscopy regarding the signal to noise
87 ratio at equal data acquisition times [19].

88 β -Lactoglobulin (β -LG) is a predominantly β -sheet protein consisting of 162 amino acids
89 that are folded in three α -helices and nine strands of antiparallel β -sheet, that are wrapped in a
90 way to form an antiparallel β -barrel [20,21]. It is a main constituent of bovine milk and therefore
91 it has been the subject of many studies probing its function and structure in relation to internal
92 and external perturbation factors such as protein concentration [22-24], temperature [25-27],
93 pressure [28], pH [21,29], ionic strength [30], denaturant concentration [31,32], metal ion
94 concentration [33], among others. In this regard, it has been found that β -LG features multiple
95 structural transitions along the entire pH range. The monomeric structure of β -LG prevailing at
96 low pH values starts to dimerize at pH 3. Between pH 4 and pH 5, β -LG undergoes a dimer-to-
97 octamer transition. Throughout these transitions taking place in the acidic pH range, the global
98 secondary structure of the antiparallel β -barrel does not show evident changes [24]. Further
99 increase of the pH value into the alkaline region leads to disruption of the β -sheet secondary
100 structure and formation of disordered secondary structure, as investigated by circular dichroism
101 (CD) spectroscopy [21] and FTIR spectroscopy [34]. Moreover, conformational changes of β -LG
102 induced by pH [24], concentration [35], temperature [25,28,36], pressure [25,28] as well as
103 adsorption [37] were successfully evaluated by FTIR spectroscopy.

104 Multivariate curve resolution-alternating least square (MCR-ALS) is a widespread
105 iterative soft-modelling technique that allows to discriminate individual contributions of
106 underlying constituents [38,39]. MCR-ALS provides sound and meaningful models with
107 chemically interpretable output in the form of spectral profiles of the compounds and the related
108 abundance distribution profiles along the dynamic process. Due to its flexibility and robustness, it
109 has been successfully used in combination with various analytical techniques, such as
110 chromatography [40], electrophoresis [41], and flow analysis [42], among others. In combination

111 with spectroscopic techniques, particularly with IR spectroscopy, MCR-ALS has become a
112 highly valuable technique for the study of evolving processes [13,43,44].

113 In this work, we present a continuous flow-through titration to monitor pH-induced
114 protein unfolding by EC-QCL-based IR spectroscopy. This type of experiment was impeded with
115 conventional FTIR spectroscopy due to experimental problems such as defects in liquid tightness
116 and cell clogging arising from the necessity of the low path length required for IR measurements
117 of proteins in aqueous solution. To this end, β -LG was chosen as a model protein as it depicts a
118 gradual transition from β -sheet to random secondary structure in the alkaline pH range. MCR-
119 ALS analysis was utilized to obtain pure spectral and abundance distribution profiles of the pH-
120 induced transition between native and denatured secondary structure.

121

122 **2. Materials and methods**

123 **2.1. Reagents and Samples**

124 Sodium hydroxide (NaOH) solution 50 % in water, potassium chloride (KCl) p.a. and β -
125 lactoglobulin (β -LG) from bovine milk (≥ 85 %) were obtained from Sigma-Aldrich (Steinheim,
126 Germany) and used as purchased. Ultrapure water (18 M Ω) was used for preparation of all
127 solutions and was obtained with a Milli-Q water purification system from Millipore (Bedford,
128 USA).

129

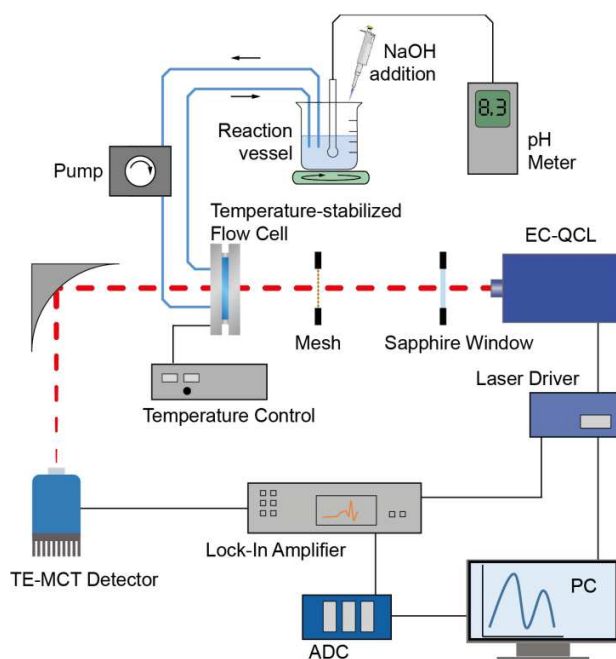
130 **2.2. EC-QCL Setup**

131 A detailed description of the custom-made EC-QCL setup can be found elsewhere [19].
132 Briefly, a water-cooled external-cavity quantum cascade laser (Hedgehog, Daylight Solutions
133 Inc., San Diego, USA) was used operating at a repetition rate of 100 kHz and a pulse width of

134 5 μ s. Spectra were recorded in the spectral tuning range of 1730–1470 cm^{-1} , covering the amide I
135 and amide II region of proteins, at a scan speed of 1200 $\text{cm}^{-1}\text{s}^{-1}$. The mid-IR light was focused on
136 the detector element by a gold plated off-axis parabolic mirror with a focal length of 43 mm. A
137 thermoelectrically-cooled MCT detector operating at $-78\text{ }^\circ\text{C}$ (PCI-10.6, Vigo Systems S.A.,
138 Poland) was used as IR detector, as shown in Fig. 1. All measurements were carried out using a
139 custom-built, temperature-controlled flow cell equipped with two mid-IR transparent CaF_2
140 windows and 31 μm -thick spacer, at $25\text{ }^\circ\text{C}$. A mesh was employed to attenuate the laser intensity
141 and a wedged sapphire window (2.5 mm thickness) was used to selectively reduce the laser
142 intensity in the amide II region. To reduce the influence of water vapor, the setup was placed in a
143 housing of polyethylene foil and constantly flushed with dry air.

144 The measured signal was processed by a lock-in amplifier (Stanford Research Systems,
145 CA, USA) and digitized by a NI DAQ 9239 24-bit ADC (National Instruments Corp., Austin,
146 USA). Each single beam spectrum consisting of 6000 data points was recorded during the tuning
147 time for one scan of approx. 250 μ s. A total of 100 scans were recorded for background and
148 sample single beam spectra at a total acquisition time of 53 s.

149 A data processing routine was devised to remove those scans that are shifted more than
150 0.1 cm^{-1} based on evaluation of the similarity index. Using this approach, approximately 3 % of
151 the recorded scans were sorted out. At last, minor Fourier filtering (cutoff frequency of 150–200)
152 was applied to remove residual noise in the final absorption spectra.



153
 154 **Fig. 1.** Experimental setup for pH titration monitored by EC-QCL IR transmission spectroscopy.
 155

156 2.3. Titration Procedure

157 400 mg of β -LG were dissolved in 20 mL of water to obtain a protein solution of
 158 20 mg mL^{-1} . Subsequently, the pH value was adjusted to 6.0 by addition of HCl. KCl (final
 159 concentration: 100 mmol L^{-1}) was added for stabilization of the ionic strength throughout the
 160 titration. pH measurements were carried out using a pH330i (Wissenschaftlich-Technische
 161 Werkstätten GmbH, Weilheim, Germany) potentiometer equipped with a Sentix® Mic-D
 162 (Wissenschaftlich Technische Werkstätten GmbH, Weilheim, Germany) combined glass
 163 electrode and temperature probe. pH titration was performed by adding $10 \mu\text{L}$ aliquots of 1 M,
 164 2.5 M, 5 M, 10 M and 15.4 M NaOH to 20 mL of the original protein solution to achieve pH
 165 increments of approximately 0.1-0.3 between spectra acquisition. In total, 37 IR spectra were
 166 obtained covering the pH range from 6.0 to pH 12.7. The solution was continuously pumped
 167 through the IR transmission cell with a pump speed of 0.9 mL min^{-1} and stopped while recording

168 of the IR spectra. The temperature was monitored throughout the titration, being constant in the
169 range of ± 0.1 °C.

170 For assessing the changes of the HOH-bending band of water throughout the introduced
171 pH change, a similar titration procedure was performed with 20 mL of medium solution,
172 constituted by water containing 100 mmol L⁻¹ of KCl. Here, 35 IR spectra were obtained between
173 pH 6.0 and pH 12.9.

174 For the calculation of all absorption spectra, ultrapure water was taken as a reference.

175

176 2.4. MCR-ALS

177 MCR-ALS is a soft-modelling iterative method that focuses on bilinear decomposition of
178 a data matrix into two submatrices containing chemically meaningful information of
179 contributions of the pure compounds involved in the system [45]. In spectroscopy, the
180 decomposition results provide information about spectral behavior of the individual sample
181 constituents and the related abundance. Here, the MCR-ALS modelling approach was chosen,
182 because it is capable to provide chemically interpretable profiles from a bilinear decomposition of
183 a unique matrix. The majority of bilinear decomposition algorithms are used with quantitative
184 aims and do not offer the possibility to reveal spectral information of the system constituents.
185 Thus, MCR-ALS seems to be the best option to unravel the spectral and chemical behavior of the
186 present system.

187 One of the most compelling characteristics of MCR-ALS resolution is its general
188 applicability without prior information about the system under study. However, to achieve
189 chemically meaningful component profiles, additional knowledge can be incorporated [46]. This
190 information can be introduced either as initial estimates of the iterative optimization or through

191 the implementation of chemical or mathematical constraints, such as non-negativity, unimodality,
192 normalization and closure, among others [47].

193 In the present work, pH-induced conformational change was monitored in the amide I and
194 amide II spectral region by varying the pH value between 6.0 and 12.7. For a complete titration
195 experiment, 37×4451 and 35×4451 matrices were obtained for protein and medium solution,
196 respectively, and subjected to MCR-ALS analysis.

197

198 **2.5. Software**

199 Data processing and MCR-ALS analysis were performed in MATLAB R2014
200 (MathWorks, Inc., Natick, MA, 2014). MCR-ALS algorithms were implemented by using MCR-
201 ALS GUI 2.0 graphical interface available at <http://www.mcrals.info>. Discrete wavelet transform
202 was implemented by using the wavelet package allocated into MATLAB R2014.

203 Daylight Solution driver software (Hedgehog, Daylight Solutions Inc., San Diego, USA)
204 was used for laser control. For data acquisition and temperature control a custom-made LabView-
205 based GUI (National Instruments Corp., Austin, USA) was utilized.

206

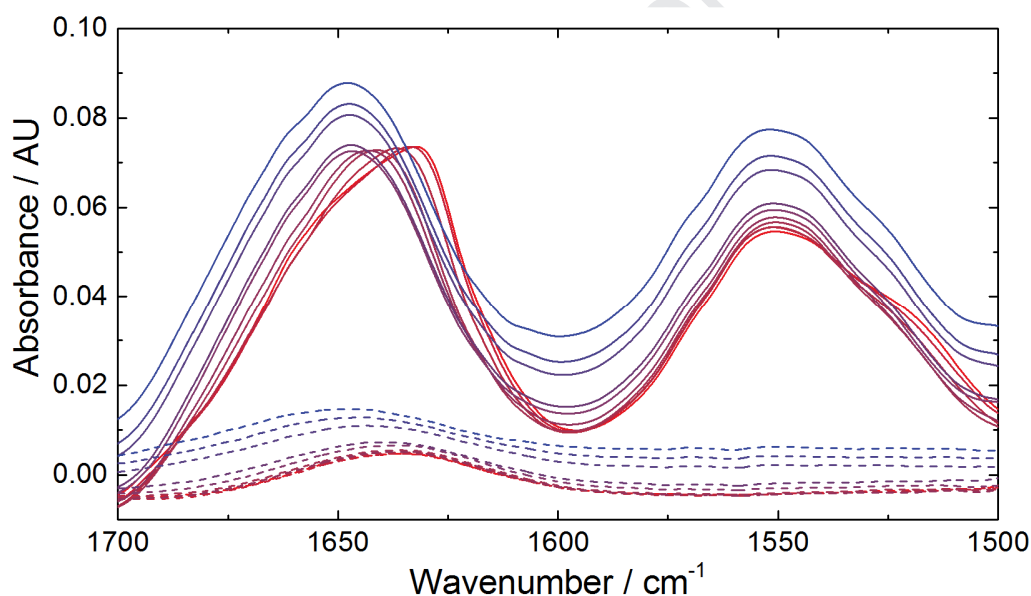
207 **3. Results and Discussion**

208 **3.1. IR Spectra of pH-induced Conformational Change of β -Lactoglobulin**

209 QCL-IR spectra of the pH-induced change of β -LG were recorded between pH 6.0 and
210 pH 12.7. In Fig. 2, the QCL-IR absorption spectra in the amide I and amide II region are shown.
211 The QCL-IR spectra at pH 6.0 shows a band maximum in the amide I region at 1634 cm^{-1} with a
212 shoulder at 1655 cm^{-1} , and a broad band at approximately 1550 cm^{-1} with a shoulder at 1520 cm^{-1}
213 in the amide II region, characteristic for the IR signatures of β -LG featuring a predominantly β -
214 sheet secondary structure [5,48]. Upon stepwise increase of the pH value, the maximum of the

215 amide I band is shifted towards higher wavenumbers and the band shape loses its distinctive
 216 form. The IR spectrum at the highest measured pH value shows broad featureless bands with
 217 maxima at 1645 cm^{-1} and 1550 cm^{-1} in the amide I and amide II region, respectively, indicating a
 218 disordered secondary structure [1,34]. Even though α -helical structure is present in β -LG, no
 219 bands could be attributed to this type of secondary structure in the recorded data set, presumably
 220 because the induced conformational change is minor compared to the pronounced transition from
 221 β -sheet to disordered secondary structure.

222



223

224 **Fig. 2.** Fourier-filtered QCL-IR spectra of 20 mg mL^{-1} β -LG recorded as a function of pH
 225 between 6.0 (red solid line) and 12.9 (blue solid line) and QCL-IR spectra of water recorded as a
 226 function of pH between 6.0 (red dashed line) and 12.7 (blue dashed line).

227

228 After reaching the end point of titration at high pH value, HCl was added to test the
 229 reversibility of the conformational change however no spectral changes were observed,
 230 suggesting the irreversibility of protein unfolding reaction (data not shown) [49].

231 Fig. 2 also shows the spectral changes of the medium (100 mmol L⁻¹ KCl) induced by the
232 variation of the pH value. The spectra reveal an absorption band at 1633 cm⁻¹ attributed to KCl-
233 solvated water [50], as well as an increasing drift of the baseline at higher pH values [51].
234 Consequently, the pH-induced change of the protein secondary structure in the IR spectra is
235 superimposed by spectral changes of the medium solution, which hampers direct analysis of the
236 dynamics of the conformational change. Consequently, MCR-ALS analysis was performed for
237 in-depth analysis of the presented pH-resolved IR spectra and further evaluation of the
238 conformational changes.

239 **3.2. Chemometric Analysis by MCR-ALS**

240 Detailed chemometric analysis of the recorded IR spectra was performed by applying
241 MCR-ALS. This approach has been successfully employed for the analysis of the progression of
242 protein secondary structural change in dynamic spectroscopic data [4,13,52].

243 For the analysis of complex systems by MCR-ALS, several aspects ought to be
244 considered in order to achieve reliable and meaningful results. One consideration relates to the
245 initialization of the ALS step. Here, the number of components involved in the system and their
246 initial estimates are required. The number of components refers to the spectroscopically active
247 species that explain the system and is usually unknown, therefore, it is estimated by applying
248 singular value decomposition (SVD) or principal component analysis (PCA). Regarding ALS
249 initialization, different first estimates can be used to initiate the modelling. The initial spectral
250 profiles can either reflect the system under study or comprise fully random values. In the first
251 mentioned case, if no spectral information of the pure constituents is available, they can be
252 estimated by means of different methodologies, such as the analysis of the purest variables [53]
253 or the so-called Evolving Factor Analysis (EFA) [54]. Even though it is reported that the nature
254 of the initial estimates does not significantly affect the final result of chemometric modelling

255 [55], it has been demonstrated that estimates closer to the real information aids achieving the true
256 solution in systems of unknown composition or of extremely complex nature [56]. For evaluation
257 of an evolving system, e.g., protein conformation monitoring in aqueous medium by IR
258 spectroscopy, the estimation of the initial profiles becomes challenging since no information
259 about system composition and information of pure constituents are available in advance.

260 In pH-titration experiments, a challenge for chemometric modelling of the system is that
261 not only the analyte but also the medium undergoes spectral changes induced by alteration of the
262 pH value, which depend on the surrounding media, among other parameters. This phenomenon,
263 which can be observed in the form of changes in the offset of the baseline or in the band position
264 and shape, arises from the concentration of ions that modify the pH (H^+ and OH^-) as well as the
265 solvation of the ions, KCl in the present case, by the water molecules. This effect can be seen in
266 Fig. 2, where absorption spectra of the medium at different pH are depicted (absorption spectra of
267 the medium were obtained against pure water). In the case of protein titration, the spectral
268 changes of the medium are overshadowed by protein signals, which are more intense than the
269 ones of the medium, precluding the proper extraction of the profiles of all constituents by
270 chemometric decomposition.

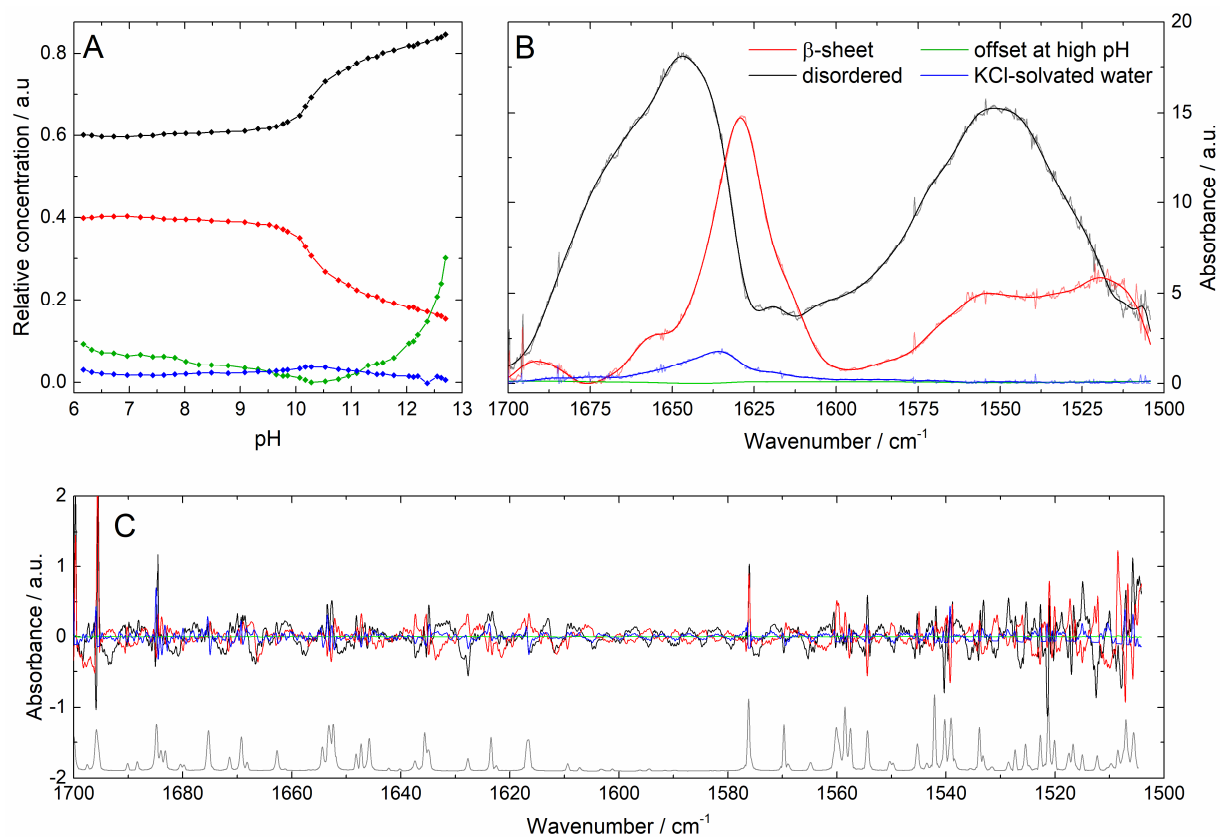
271 In the context of this complex scenario, the following procedure was implemented in the
272 attempt to extract the most reliable, accurate and representative information about the system. For
273 MCR-ALS analysis, un(Fourier-)filtered QCL-IR spectra were employed. First, medium-titration
274 and protein-titration data were individually subjected to MCR-ALS analysis. In both cases, the
275 optimum number of components that explain the system estimated by SVD was evaluated to be
276 three and four, respectively. Abundance distribution profiles obtained from the analysis of the
277 purest variables to each individual data set were utilized as initial estimates of the ALS
278 optimization. For the medium system, non-negativity and spectra normalization constraints were

279 implemented, while for the protein system, non-negativity, spectra normalization and closure for
280 those components involved in the protein evolution were applied. Once the optimized results
281 were obtained from the separate analyses, the optimized spectral profiles were combined in order
282 to build a unique set of spectral profiles. It should be noted that two of the spectral profiles
283 obtained from the protein titration analysis correspond to the medium. Subsequently, those
284 profiles were replaced with the profiles obtained from the medium-titration analysis. Therefore,
285 five optimized spectral profiles were assembled into a matrix, two for the protein (obtained from
286 protein analysis) and three for the medium (obtained from the medium analysis), and were
287 considered as initial estimates for a subsequent extended MCR-ALS analysis of an augmented
288 data matrix.

289 The augmented data matrix was built by appending the original medium data matrix to the
290 protein data matrix. In this way, a 72×4451 data matrix was obtained and analyzed by the
291 extended version of MCR-ALS. Here, the previously obtained five optimized spectral profiles
292 were utilized as initial estimates of the ALS step. Non-negativity and spectra normalization were
293 implemented as constraints during optimization. In this manner, it was possible to model the
294 contribution of the medium in presence of protein. It is a pronounced benefit of the employed
295 extended MCR-ALS modelling to analyze the reference and the sample matrix in one single
296 model. This is in particular the case for pH titrations, where pH levels cannot be exactly
297 reproduced for the reference and sample titration. Consequently, absorption spectra at individual
298 pH values cannot be directly calculated without introducing spectral artefacts due to pH
299 differences between the reference and sample spectrum. Figure 3 shows the optimized results
300 achieved by MCR-ALS analysis for the protein evolution through the pH variation.

301 The MCR-ALS analysis resolved pH-dependent (Fig. 3A) and spectral profiles (Fig. 3B)
302 of the protein secondary structures as well as spectral elements of the medium that change with

303 increasing pH value. The spectral profile attributed to the β -sheet secondary structure features a
 304 band maximum at 1630 cm^{-1} in the amide I region and a prominent shoulder around 1520 cm^{-1} in
 305 the amide II region (Fig. 3B). The component attributed to the disordered protein structure shows



306
 307
 308 **Fig. 3.** (A) pH-dependent and (B) spectral profiles retrieved by MCR-ALS for the performed pH-
 309 titration of β -lactoglobulin at a concentration of 20 mg mL^{-1} and the pH-titration of the medium.
 310 The red and black lines show the β -sheet and disordered secondary structure of the protein,
 311 respectively. The green lines indicate the offset of the baseline at elevated pH values and the blue
 312 lines exhibit the contribution of KCl-solvated water. Thin lines in (B) are raw spectral profiles
 313 received by MCR-ALS, thick lines in (B) were obtained by discrete Meyer wavelet transform

314 (WT). (C) Residuals obtained from the WT for the individual spectral profiles. The grey line
315 shows a (scaled) spectrum of water vapor.

316

Journal Pre-proof

317 band maxima at 1645 cm^{-1} and 1550 cm^{-1} in the amide I and amide II region, respectively. The
318 shapes and maximum positions of the spectral profiles obtained by rigorous application of MCR-
319 ALS analysis fit well to spectral features reported for IR spectra of the respective secondary
320 structure elements. The profiles of the pH-dependent evolution of the two secondary structures
321 (Fig. 3A) reveal that the respective share remains constant between pH 5.0 and 9.5. Upon further
322 increase of the pH value, the fraction of β -sheet secondary structure rapidly decreases while the
323 portion of disordered protein structure increases in the same manner with an inflection point at
324 pH ~ 10.2 . Above pH 11, the rapid conversion of secondary structure is completed, and the
325 change continues at slower and constant rate. This progression of pH induced conversion of β -LG
326 secondary structure agrees well with reported results obtained by CD spectroscopy [21].

327 The MCR-ALS analysis further revealed pH-dependent (Fig. 3A) and spectral profiles
328 (Fig. 3B) of the medium constituents. One spectral profile with a maximum at 1634 cm^{-1} was
329 attributed to the absorption of KCl-solvated water. This assignment seems reasonable, as the KCl
330 concentration does not change throughout the titration, which is reflected in the constant and flat
331 progression in the pH-dependent profiles (Fig. 3A). Finally, the fourth, rather featureless spectral
332 profile is attributed to the baseline offset in IR spectra that occurs in aqueous solutions at elevated
333 pH values. This is supported by the significant increase of the relative concentration of this
334 spectral profile at pH > 11.5 . The fifth retrieved component (not shown) does not demonstrate
335 any particular spectral feature and then could not be attributed to a specific phenomenon;
336 however, it was necessary to include to improve the goodness of fit of the MCR-ALS model.

337

338

339

340

341

342 **3.3. Evaluation of spectral profiles**

343 In the previous section, MCR-ALS was employed for chemometric analysis of QCL-IR
344 spectra monitoring the conformational change during pH titration. However, chemometric
345 analysis also allows to retrieve additional in-depth information of the experimentally recorded
346 QCL-IR spectra and reveal details about the experimental setup.

347 At this point, it should be emphasized that for chemometric models such as MCR-ALS,
348 any characteristic of the analyzed data is of paramount interest and will influence the obtained
349 result. In this regard, the noise plays an important role in the decomposition. In most cases, the
350 noise in the experimental data is introduced by stochastic variations of the system, for example,
351 instrumental and electrical interferences, and consequently presents a random behavior. To
352 facilitate the modelling, random noise can be abolished by implementing denoising procedures,
353 such as Savitzky-Golay smoothing. On the other hand, advanced denoising procedures, as
354 transforms or filtering, may disrupt the random structure of the noise and, then, change the inner
355 structure of the data turning the random into non-random noise. Besides, either smoothing or
356 filtering is not trivial to implement and distortions can be unintentionally introduced to the
357 original signals, which would alter the information comprised in the experimental data. For
358 illustration, Figure S1 shows the results obtained from the MCR-ALS analysis of (Fourier
359 transform) FT-filtered data. It can be observed that only one component was obtained for the
360 medium and the spectral profiles of the protein and the medium are distorted in comparison to the
361 results obtained from the unfiltered data resolution.

362 Moreover, the experimental data may also contain non-random noise contributions. For
363 example, it is known that spectra obtained by EC-QCL based setups may contain, besides the
364 intrinsic random noise, a fine structure originating from the mode-hops due to competition of

365 different optical modes for the available net gain in the laser medium [57]. Furthermore, the
366 numerous optical components of optical setups may introduce periodic spectral features due to
367 fringing effects. For this reason, no denoising procedures were implemented prior to MCR-ALS
368 modelling in order to avoid equivocal results due to artefacts introduced by the denoising step.

369 After MCR-ALS, a denoising procedure was carefully selected, to decompose the
370 spectroscopic signal from the non-random noise components of the experimental data.
371 Consequently, discrete Meyer wavelet transform (MWT) was applied to denoise the retrieved
372 spectral profiles. Fig. 3B shows a comparison of the raw spectral profiles retrieved by MCR-ALS
373 before and after denoising by MWT and Fig. 3C depicts the residuals obtained from the MWT.
374 Analysis of residuals reveals the presence of low band-width spikes in the spectral profiles that
375 can be attributed to the characteristic bands of water vapor. Since the entire titration procedure
376 requires approximately five hours, it is experimentally difficult to maintain the same humidity
377 throughout this time period. Furthermore, beside the stochastic noise, interference fringes are
378 present in the entire spectral region and recognizable particularly well in the region between
379 $1580\text{-}1615\text{ cm}^{-1}$, that is undisturbed by water vapor gas-phase bands. Interference fringes are
380 sinusoidal pattern on the baseline of the spectrum caused by interference between radiation that
381 has been transmitted directly through an optical element such as windows or sample cells with
382 light that has been reflected internally. Furthermore, the decreasing amplitude of the interference
383 fringes with increasing wavenumbers indicates that the surfaces are not perfectly parallel [58].
384 Within the experimental setup, this kind of fringes can stem for example from sample cell
385 windows or the Sapphire window employed for attenuating the laser power in the amide II region
386 [19].

387

388 **4. Conclusion**

389 EC-QCL based IR transmission spectroscopy was applied for performing a titration to monitor
390 the pH-induced conformational change of β -lactoglobulin between pH 6.0 and 12.7. The
391 experimental feasibility for this measurement was enabled by the large optical transmission path
392 applicable due to the high emission power of quantum cascade lasers. The spectra revealed a
393 change of protein secondary structure in the investigated pH region, but also an increasing offset
394 of the baseline at elevated pH values that impeded straight-forward evaluation. Consequently,
395 MCR-ALS was employed to unravel the overlapping spectral features in the IR spectra. With this
396 chemometric technique, spectral and abundance distribution profiles were obtained by analysis of
397 recorded dynamic IR spectra. Spectral profiles obtained by the MCR-ALS model for the
398 identified secondary structure elements show good comparability with recorded IR spectra
399 regarding band positions. The abundance distribution profiles reveal a transition from β -sheet to
400 disordered secondary structure with a transition point at a pH value of ~ 10.2 , which is in
401 accordance to previously reported investigations of this system by CD spectroscopy. In addition,
402 wavelet transform was successfully implemented to the MCR-ALS spectral profiles allowing to
403 extract significant information about the spurious signals that are intrinsically present in QCL-IR
404 spectra.

405 In conclusion, the present study demonstrates that laser-based IR transmission
406 spectroscopy is an excellent tool for performing flow-through measurements of proteins in
407 aqueous solution. Furthermore, it was demonstrated that MCR-ALS in combination with IR
408 spectroscopy is a powerful technique for monitoring and interpreting protein folding.

409

410 **Acknowledgements**

411 This work has received funding from the European Union's Horizon 2020 research and
412 innovation programme under grant agreement No. 780240. M.R.A. acknowledges CONICET for
413 her postdoc fellowship.

414

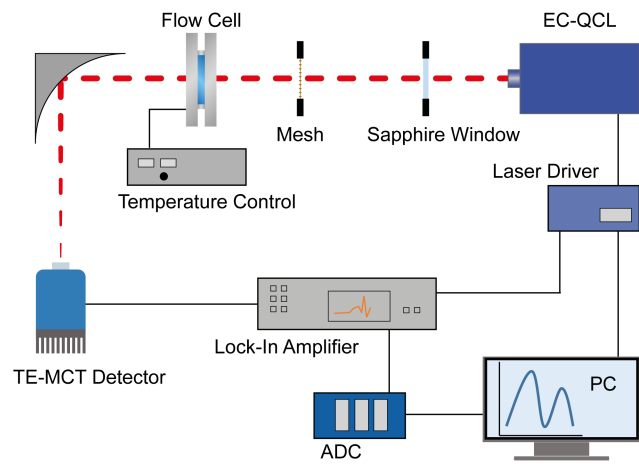
415 **References**

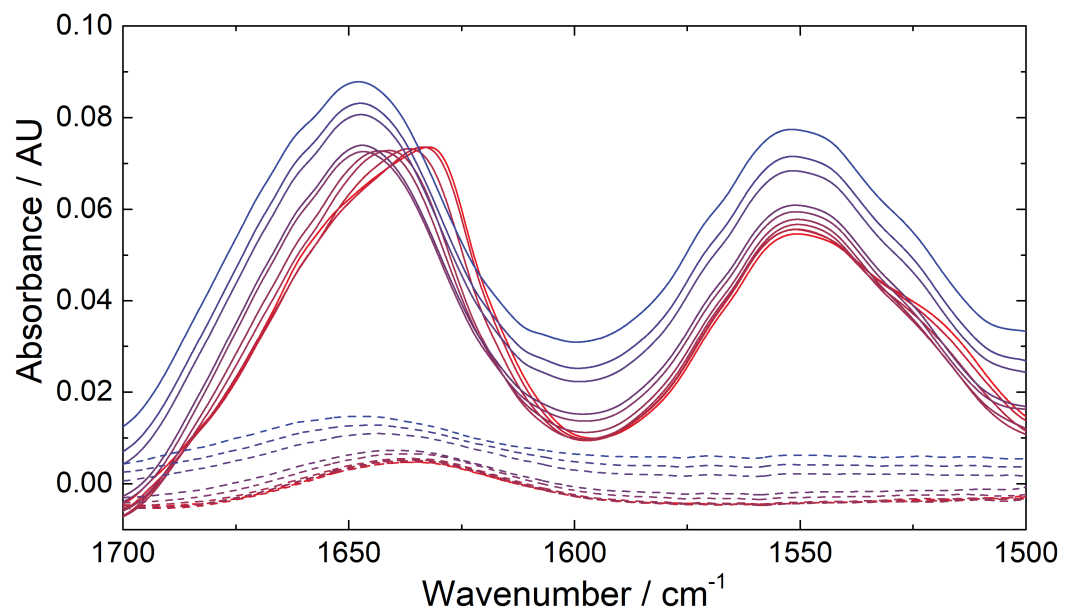
- 416 [1] A. Barth, Infrared spectroscopy of proteins, *Biochim. Biophys. Acta, Bioenerg.* 1767
417 (2007) 1073-1101.
- 418 [2] M.C. Manning, Use of infrared spectroscopy to monitor protein structure and stability,
419 *Expert Rev. Proteomics* 2 (2005) 731-743.
- 420 [3] S. Bal Ram, Basic Aspects of the Technique and Applications of Infrared Spectroscopy of
421 Peptides and Proteins, in: *Infrared Analysis of Peptides and Proteins*, American Chemical
422 Society, 1999, pp. 2-37.
- 423 [4] M.R. Alcaráz, A. Schwaighofer, H. Goicoechea, B. Lendl, Application of MCR-ALS to
424 reveal intermediate conformations in the thermally induced α - β transition of poly-L-lysine
425 monitored by FT-IR spectroscopy, *Spectrochim. Acta, Part A* 185 (2017) 304-309.
- 426 [5] F. Dousseau, M. Pezolet, Determination of the secondary structure content of proteins in
427 aqueous solutions from their amide I and amide II infrared bands. Comparison between classical
428 and partial least-squares methods, *Biochemistry* 29 (1990) 8771-8779.
- 429 [6] S. Navea, R. Tauler, E. Goormaghtigh, A. de Juan, Chemometric tools for classification
430 and elucidation of protein secondary structure from infrared and circular dichroism spectroscopic
431 measurements, *Proteins: Struct., Funct., Genet.* 63 (2006) 527-541.
- 432 [7] H. Fabian, W. Mäntele, *Infrared Spectroscopy of Proteins*, in: *Handbook of Vibrational*
433 *Spectroscopy*, John Wiley & Sons, Ltd, Hoboken, NJ, USA, 2006.
- 434 [8] C. Zscherp, A. Barth, Reaction-Induced Infrared Difference Spectroscopy for the Study of
435 Protein Reaction Mechanisms, *Biochemistry* 40 (2001) 1875-1883.
- 436 [9] J. Faist, F. Capasso, D.L. Sivco, C. Sirtori, A.L. Hutchinson, A.Y. Cho, Quantum Cascade
437 Laser, *Science* 264 (1994) 553-556.
- 438 [10] M.J. Weida, B. Yee, Quantum cascade laser-based replacement for FTIR microscopy,
439 *Proc. Soc. Photo-Opt. Instrum. Eng.* 7902 (2011) 79021C.
- 440 [11] A. Schwaighofer, M. Brandstetter, B. Lendl, Quantum cascade lasers (QCLs) in
441 biomedical spectroscopy, *Chem. Soc. Rev.* 46 (2017) 5903-5924.
- 442 [12] M.R. Alcaráz, A. Schwaighofer, C. Kristament, G. Ramer, M. Brandstetter, H.
443 Goicoechea, B. Lendl, External cavity-quantum cascade laser spectroscopy for mid-IR
444 transmission measurements of proteins in aqueous solution, *Anal. Chem.* 87 (2015) 6980-6987.
- 445 [13] M.R. Alcaráz, A. Schwaighofer, H. Goicoechea, B. Lendl, EC-QCL mid-IR transmission
446 spectroscopy for monitoring dynamic changes of protein secondary structure in aqueous solution
447 on the example of beta-aggregation in alcohol-denatured alpha-chymotrypsin, *Anal. Bioanal.*
448 *Chem.* 408 (2016) 3933-3941.
- 449 [14] A. Schwaighofer, M.R. Alcaráz, C. Araman, H. Goicoechea, B. Lendl, External cavity-
450 quantum cascade laser infrared spectroscopy for secondary structure analysis of proteins at low
451 concentrations, *Sci. Rep.* 6 (2016) 33556.

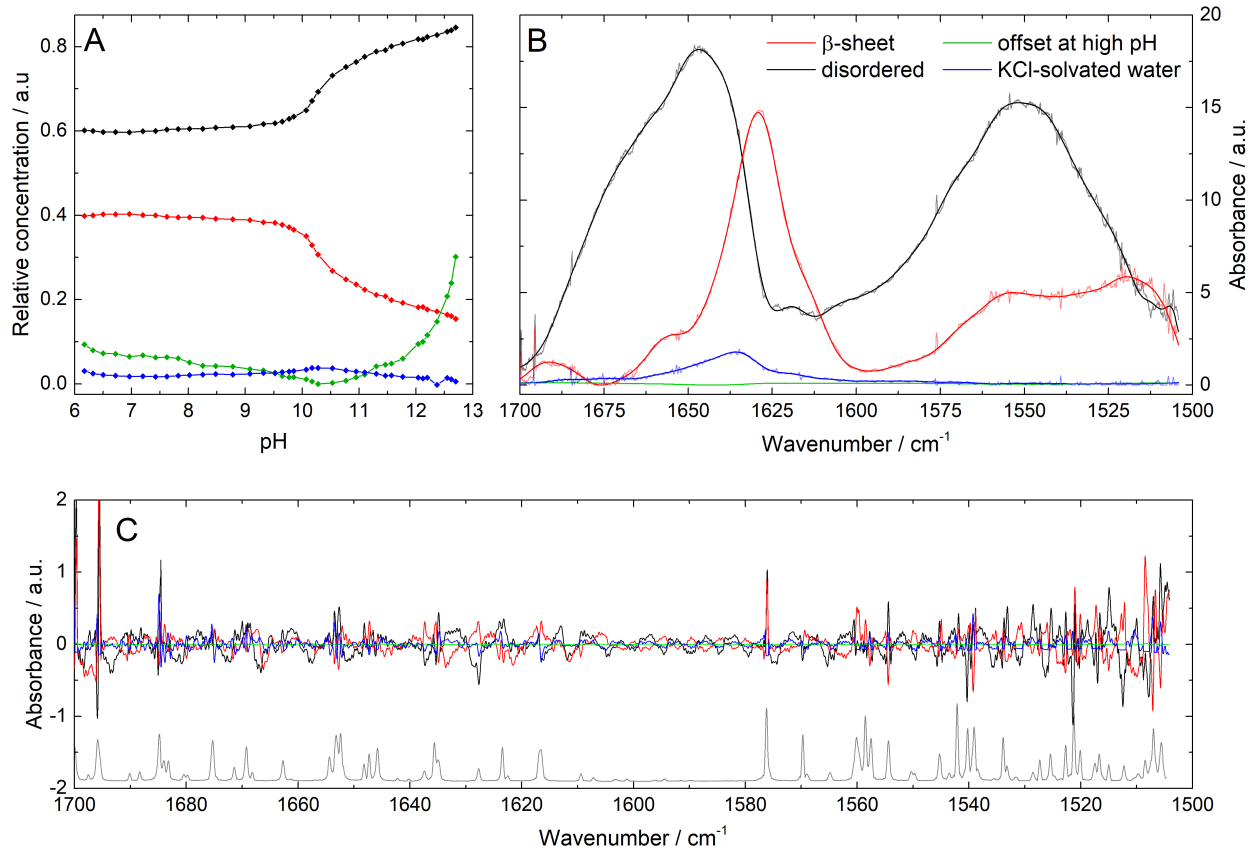
- 452 [15] D.J. Wurm, J. Quehenberger, J. Mildner, B. Eggenreich, C. Slouka, A. Schwaighofer, K.
453 Wieland, B. Lendl, V. Rajamanickam, C. Herwig, O. Spadiut, Teaching an old pET new tricks:
454 tuning of inclusion body formation and properties by a mixed feed system in *E. coli*, *Appl.*
455 *Microbiol. Biotechnol.* 102 (2018) 667-676.
- 456 [16] J. Kuligowski, A. Schwaighofer, M.R. Alcaráz, G. Quintás, H. Mayer, M. Vento, B.
457 Lendl, External cavity-quantum cascade laser (EC-QCL) spectroscopy for protein analysis in
458 bovine milk, *Anal. Chim. Acta* 963 (2017) 99-105.
- 459 [17] A. Schwaighofer, J. Kuligowski, G. Quintás, H.K. Mayer, B. Lendl, Fast quantification of
460 bovine milk proteins employing external cavity-quantum cascade laser spectroscopy, *Food*
461 *Chem.* 252 (2018) 22-27.
- 462 [18] A. Schwaighofer, M.R. Alcaráz, J. Kuligowski, B. Lendl, Recent advancements of EC-
463 QCL based mid-IR transmission spectroscopy of proteins and application to analysis of bovine
464 milk, *Biomed. Spectrosc. Imaging* 7 (2018) 35-45.
- 465 [19] A. Schwaighofer, M. Montemurro, S. Freitag, C. Kristament, M.J. Culzoni, B. Lendl,
466 Beyond FT-IR spectroscopy: EC-QCL based mid-IR transmission spectroscopy of proteins in the
467 amide I and amide II region, *Anal. Chem.* 90 (2018) 7072-7079.
- 468 [20] A. Dong, J. Matsuura, S.D. Allison, E. Chrisman, M.C. Manning, J.F. Carpenter, Infrared
469 and circular dichroism spectroscopic characterization of structural differences between beta-
470 lactoglobulin A and B, *Biochemistry* 35 (1996) 1450-1457.
- 471 [21] N. Taulier, T.V. Chalikian, Characterization of pH-induced transitions of beta-
472 lactoglobulin: Ultrasonic, densimetric, and spectroscopic studies, *J. Mol. Biol.* 314 (2001) 873-
473 889.
- 474 [22] X.L. Qi, S. Brownlow, C. Holt, P. Sellers, Thermal-Denaturation of Beta-Lactoglobulin -
475 Effect of Protein-Concentration at Ph-6.75 and Ph-8.05, *Biochim. Biophys. Acta, Protein Struct.*
476 *Mol. Enzymol.* 1248 (1995) 43-49.
- 477 [23] B. Czarnik-Matusiewicz, K. Murayama, Y.Q. Wu, Y. Ozaki, Two-dimensional attenuated
478 total reflection/infrared correlation spectroscopy of adsorption-induced and concentration-
479 dependent spectral variations of beta-lactoglobulin in aqueous solutions, *J. Phys. Chem. B* 104
480 (2000) 7803-7811.
- 481 [24] J.C. Ioannou, A.M. Donald, R.H. Tromp, Characterising the secondary structure changes
482 occurring in high density systems of BLG dissolved in aqueous pH 3 buffer, *Food Hydrocolloids*
483 46 (2015) 216-225.
- 484 [25] S. Ngarize, H. Herman, A. Adams, N. Howell, Comparison of changes in the secondary
485 structure of unheated, heated, and high-pressure-treated ss-lactoglobulin and ovalbumin proteins
486 using Fourier transform Raman spectroscopy and self-deconvolution, *J. Agr. Food Chem.* 52
487 (2004) 6470-6477.
- 488 [26] C. Le Bon, T. Nicolai, D. Durand, Growth and structure of aggregates of heat-denatured
489 beta-Lactoglobulin, *Int. J. Food Sci. Technol.* 34 (1999) 451-465.
- 490 [27] P. Havea, H. Singh, L.K. Creamer, Characterization of heat-induced aggregates of beta-
491 lactoglobulin, alpha-lactalbumin and bovine serum albumin in a whey protein concentrate
492 environment, *J. Dairy Res.* 68 (2001) 483-497.
- 493 [28] G. Panick, R. Malessa, R. Winter, Differences between the Pressure- and Temperature-
494 Induced Denaturation and Aggregation of β -Lactoglobulin A, B, and AB Monitored by FT-IR
495 Spectroscopy and Small-Angle X-ray Scattering, *Biochemistry* 38 (1999) 6512-6519.
- 496 [29] S. Uhrínová, M.H. Smith, G.B. Jameson, D. Uhrín, L. Sawyer, P.N. Barlow, Structural
497 Changes Accompanying pH-Induced Dissociation of the β -Lactoglobulin Dimer^{†,‡},
498 *Biochemistry* 39 (2000) 3565-3574.

- 499 [30] Y. Yan, D. Seeman, B. Zheng, E. Kizilay, Y. Xu, P.L. Dubin, pH-Dependent Aggregation
500 and Disaggregation of Native β -Lactoglobulin in Low Salt, *Langmuir* 29 (2013) 4584-4593.
- 501 [31] V.N. Uversky, N.V. Narizhneva, S.O. Kirschstein, S. Winter, G. Lober, Conformational
502 transitions provoked by organic solvents in beta-lactoglobulin: Can a molten globule like
503 intermediate be induced by the decrease in dielectric constant?, *Folding Des.* 2 (1997) 163-172.
- 504 [32] D. Hamada, C.M. Dobson, A kinetic study of β -lactoglobulin amyloid fibril formation
505 promoted by urea, *Protein Sci.* 11 (2002) 2417-2426.
- 506 [33] G. Navarra, M. Leone, V. Militello, Thermal aggregation of beta-lactoglobulin in
507 presence of metal ions, *Biophys. Chem.* 131 (2007) 52-61.
- 508 [34] H.L. Casal, U. Kohler, H.H. Mantsch, Structural and Conformational-Changes of Beta-
509 Lactoglobulin-B - an Infrared Spectroscopic Study of the Effect of Ph and Temperature, *Biochim.*
510 *Biophys. Acta* 957 (1988) 11-20.
- 511 [35] S. Joris, I. John, T. Hans, D. Athene, S. Paul van der, Mass-action driven conformational
512 switching of proteins: investigation of beta-lactoglobulin dimerisation by infrared spectroscopy,
513 *J. Phys. D: Appl. Phys.* 48 (2015) 384001.
- 514 [36] T. Lefevre, M. Subirade, Structural and interaction properties of beta-Lactoglobulin as
515 studied by FTIR spectroscopy, *Int. J. Food Sci. Technol.* 34 (1999) 419-428.
- 516 [37] Y. Fang, D.G. Dalgleish, Conformation of beta-lactoglobulin studied by FTIR: Effect of
517 pH, temperature, and adsorption to the oil-water interface, *J. Colloid Interf. Sci.* 196 (1997) 292-
518 298.
- 519 [38] C. Ruckebusch, L. Blanchet, Multivariate curve resolution: A review of advanced and
520 tailored applications and challenges, *Anal. Chim. Acta* 765 (2013) 28-36.
- 521 [39] R. Tauler, A. de Juan, Multivariate Curve Resolution for Quantitative Analysis, in:
522 Arsenio Muñoz de la Peña, Héctor C. Goicoechea, G.M. Escandar, C.O. Alejandro (Eds.) *Data*
523 *Handling in Science and Technology*, Elsevier, 2015, pp. 247-292.
- 524 [40] M.R. Alcaráz, G.G. Siano, M.J. Culzoni, A. Munoz de la Pena, H.C. Goicoechea,
525 Modeling four and three-way fast high-performance liquid chromatography with fluorescence
526 detection data for quatitation of fluoroquinolones in water samples, *Anal. Chim. Acta* 809 (2014)
527 37-46.
- 528 [41] M.R. Alcaráz, L. Vera-Candioti, M.J. Culzoni, H.C. Goicoechea, Ultrafast quantitation of
529 six quinolones in water samples by second-order capillary electrophoresis data modeling with
530 multivariate curve resolution-alternating least squares, *Anal. Bioanal. Chem.* 406 (2014) 2571-
531 2580.
- 532 [42] M.R. Alcaráz, A.V. Schenone, M.J. Culzoni, H.C. Goicoechea, Modeling of second-order
533 spectrophotometric data generated by a pH-gradient flow injection technique for the
534 determination of doxorubicin in human plasma, *Microchem. J.* 112 (2014) 25-33.
- 535 [43] J. Diewok, A. De Juan, R. Tauler, B. Lendl, Quantitation of mixtures of diprotic organic
536 acids by FT-IR flow titrations and multivariate curve resolution, *Appl. Spectrosc.* 56 (2002) 40-
537 50.
- 538 [44] J. Kuligowski, G. Quintas, R. Tauler, B. Lendl, M. de la Guardia, Background Correction
539 and Multivariate Curve Resolution of Online Liquid Chromatography with Infrared
540 Spectrometric Detection, *Anal. Chem.* 83 (2011) 4855-4862.
- 541 [45] S.C. Rutan, A. de Juan, R. Tauler, 2.15 - Introduction to Multivariate Curve Resolution,
542 in: S.D.B.T. Walczak (Ed.) *Comprehensive Chemometrics*, Elsevier, Oxford, 2009, pp. 249-259.
- 543 [46] R. Tauler, M. Maeder, A. de Juan, Multiset Data Analysis: Extended Multivariate Curve
544 Resolution, in: S.D. Brown, R. Tauler, B. Walczak (Eds.) *Comprehensive Chemometrics:*
545 *Chemical and Biochemical Data Analysis*, Elsevier, Oxford, 2009, pp. 473-505.

- 546 [47] A. De Juan, R. Tauler, Multivariate Curve Resolution (MCR) from 2000: Progress in
547 Concepts and Applications, *Crit. Rev. Anal. Chem.* 363-4 (2006) 163-176.
- 548 [48] H.L. Monaco, G. Zanotti, P. Spadon, M. Bolognesi, L. Sawyer, E.E. Eliopoulos, Crystal-
549 Structure of the Trigonal Form of Bovine Beta-Lactoglobulin and of Its Complex with Retinol at
550 2.5-Å Resolution, *J. Mol. Biol.* 197 (1987) 695-706.
- 551 [49] L. Sawyer, β -Lactoglobulin, in: P.L.H. McSweeney, P.F. Fox (Eds.) *Advanced Dairy*
552 *Chemistry: Volume 1A: Proteins: Basic Aspects*, 4th Edition, Springer US, Boston, MA, 2013,
553 pp. 211-259.
- 554 [50] J.J. Max, C. Chapados, Interpolation and extrapolation of infrared spectra of binary ionic
555 aqueous solutions, *Appl. Spectrosc.* 53 (1999) 1601-1609.
- 556 [51] R. Vonach, B. Lendl, R. Kellner, Modulation of the pH in the determination of phosphate
557 with flow injection and Fourier transform infrared detection, *Analyst* 122 (1997) 525-530.
- 558 [52] A. Borges, R. Tauler, A.d. Juan, Application of multivariate curve resolution to the
559 temperature-induced unfolding of α -chymotrypsin, *Anal. Chim. Acta* 544 (2005) 159-166.
- 560 [53] W. Windig, J. Guilment, Interactive self-modeling mixture analysis, *Anal. Chem.* 63
561 (1991) 1425-1432.
- 562 [54] M. Maeder, A. Zilian, Evolving Factor-Analysis, a New Multivariate Technique in
563 Chromatography, *Chemometr. Intell. Lab.* 3 (1988) 205-213.
- 564 [55] A. de Juan, S.C. Rutan, R. Tauler, 2.19 - Two-Way Data Analysis: Multivariate Curve
565 Resolution – Iterative Resolution Methods, in: S.D.B.T. Walczak (Ed.) *Comprehensive*
566 *Chemometrics*, Elsevier, Oxford, 2009, pp. 325-344.
- 567 [56] M.R. Alcaraz, A. Aguirre, H.C. Goicoechea, M.J. Culzoni, S.E. Collins, Resolution of
568 intermediate surface species by combining modulated infrared spectroscopy and chemometrics,
569 *Anal. Chim. Acta.* 1049 (2019) 38-46.
- 570 [57] G. Wysocki, R.F. Curl, F.K. Tittel, R. Maulini, J.M. Bulliard, J. Faist, Widely tunable
571 mode-hop free external cavity quantum cascade laser for high resolution spectroscopic
572 applications, *Appl. Phys. B: Lasers Opt.* 81 (2005) 769-777.
- 573 [58] P.R. Griffiths, J.A. de Haseth, *Fourier Transform Infrared Spectrometry*, John Wiley &
574 Sons, Inc., Hoboken, NJ, USA, 2006.
- 575







Highlights:

- Mid-infrared (IR) External Cavity-Quantum Cascade Laser (EC-QCL) spectroscopy
- pH titration of β -lactoglobulin
- Measurement and analysis of the protein amide I and amide II region
- Evaluation by multivariate curve resolution-alternating least square (MCR-ALS)
- Unfolding of native β -sheet secondary structure at basic pH

Journal Pre-proof

Declaration of interests

The authors declare that they have no known competing financial interests or personal relationships that could have appeared to influence the work reported in this paper.

Journal Pre-proof